An Automated Thermochemistry Protocol based on Explicitly–Correlated Coupled-Cluster Theory: The Methyl- and Ethyl-peroxy Families

Bradley K. Welch,[1] Richard Dawes,[1,*] David H. Bross,[2] Branko Ruscic[2,3,*]

[1]Department of Chemistry, Missouri University of Science and Technology, Rolla, Missouri 65409, United States.

[2] Chemical Sciences and Engineering Division, Argonne National Laboratory, Argonne, Illinois 60439, United States.

[3] Consortium for Advanced Science and Engineering, University of Chicago, Chicago, Illinois 60637, United States.

Abstract

An automated computational thermochemistry protocol based on explicitly-correlated coupled-cluster theory was designed to produce highly accurate enthalpies of formation and atomization energies for small to medium-sized molecular species (3-12 atoms). Each potential source of error was carefully examined and the sizes of contributions to the total atomization enthalpies were used to generate uncertainty estimates. The protocol was first used to generate total atomization enthalpies for a family of four molecular species exhibiting a variety of charges, multiplicities, and electronic ground states. The new protocol was shown to be in good agreement with the Active Thermochemical Tables database for the four species: methylperoxy radical, methoxyoxoniumylidene (methylperoxy cation), methylperoxy anion, and methyl hydroperoxide. Updating the Active Thermochemical Tables to include those results yielded significantly improved accuracy for the formation enthalpies of those species. The derived protocol was then used to predict formation enthalpies for the larger ethyl peroxy family of species.

* corresponding author email: dawesr@mst.edu; ruscic@anl.gov

Introduction

Organic peroxide thermochemistry is important to understanding atmospheric and combustion reaction networks. The simplest organic peroxy radical, methylperoxy is an important species in the atmosphere. Methylperoxy (CH_3O_2) reacting with nitric oxide (NO) produces about 25% of all tropospheric ozone (O_3),[1] and also leads to the production of methoxy radical (CH_3O) and nitrogen dioxide (NO_2), other components of smog.[2] It also reacts with hydroperoxy radical to yield CH_3OOH, and through reaction with ROO, is a source of atmospheric methanol. A recent study showed that methylperoxy is behind the most plausible explanation for the formation of the simplest Criegee intermediate (CH_2OO, carbonyl oxide).[3] The closely related cation and anion species of the methylperoxy are also involved in some of these reactions, and therefore accurate enthalpies are desirable for the entire family of compounds.[1] Both methylperoxy and the higher ROO homologs, such as the ethylperoxy, play important roles in combustion, where under auto-ignition conditions can isomerize to QOOH, which can then further decompose to other species.[4,5,6] Unlike methylperoxy, ethylperoxy also has a notable three body dissociation channel.[4] To enable high accuracy studies of these species a comprehensive description of the thermochemistry of methylperoxy, related species, and larger peroxy species is necessary. In general, reliable data is necessary for accurate kinetics computations involving many intermediates. Relatively small errors can significantly impact computed reaction barriers and associated rates. Explicit consideration of numerous reaction steps is common in accurate models of atmospheric processes, combustion, as well as interstellar chemistry.

Composite thermochemistry calculations have been developed that offer accuracy far beyond what can be affordably achieved in any single calculation. Recent high accuracy composite methods such as the various HEAT protocols,[7,8] the W4 family,[9] as well as the FPD approach[10] offer the ability to obtain 2σ uncertainties[11] in computed 0 K enthalpies of formation less than ±1 kJ mol^{-1} in favorable cases, far exceeding the common "chemical accuracy" target of ±1 kcal/mol (~4 kJ mol^{-1}). These approaches rely on composite schemes to compute various components of the total energy separately. In general, different computational methods are applied to each contribution, which permits tuning of the overall cost and accuracy. While these composite protocols can obtain highly accurate thermochemical values, they are still challenging to use for larger species primarily due to their poor scaling with respect to the number of electrons and nuclei.

The original HEAT protocol as well as the W4 method are currently limited to small systems of only a few heavy atoms. Recent developments such as the perturbative quadruples method [CCSDT(Q)][12] as well as general improvements to computer hardware have allowed these protocols to be extended. An application of the HEAT and W4lite approaches to a medium sized molecule were reported in a study of benzene by Harding *et al.*[13] and by Karton *et al.*[14] Another direction in protocol development for larger systems involves developing scaling procedures and extrapolations to permit use of smaller bases for the most expensive terms. This is seen in methods such as the W3X, W3X-L, ANO-0, ANO-F12, diet-HEAT-F12, and mHEAT.[15-19] These approximations help control costs for larger molecules. There are several reported thermochemical protocols that employ explicitly-correlated coupled-cluster (F12) theory in some way (W1-F12,[20] W3-F12,[20] W4-F12,[21] and diet-HEAT-F12[6] are examples).

Owing to the central role of thermodynamics, there is a long history of efforts to compile the currently available thermodynamic data into tabulations usable by the broader scientific community. The nature of these lists is reviewed in detail elsewhere,[22] but even the best critically evaluated compilation has the severe limitation that it cannot be easily updated with new information because of the nature of their sequential construction. Traditional thermochemical determinations are also usually based upon a single set of experiments or computational result. In a departure from this, the Active Thermochemical Tables approach (ATcT) of Ruscic *et al.*[23,24] enables seamless updates and uses all of the available information to yield a self-consistent set of thermochemical values. The ATcT approach relies on construction of the thermochemical network (TN) from all determinations and self-consistently solves the TN leading to more accurate set of thermodynamic values.[23-25] ATcT has driven down the uncertainty for most species contained within it to at least an order of magnitude better than previous efforts, with small molecules having uncertainties frequently less than ±1 kJ mol^{-1} and in some cases below ±0.1 kJ mol^{-1}.[25] Through this reduction in uncertainty, ATcT has in turn provided the critical benchmarks that are necessary prerequisites for developing new high accuracy composite methods. To streamline the generation of accurate thermochemical data for these and other species, and to facilitate their introduction to the ATcT network, we have developed an automated computational workflow. Based on explicitly-correlated coupled-cluster theory, and governed by Python scripts, the protocol was developed and benchmarked through application to the methylperoxy family of species, validated

through consistency with the existing ATcT database as well as other experimental and computational results.

Computational Details

A complete composite method necessarily includes all contributions that are significant within the desired accuracy for the species of interest. Since the desired accuracy target here is to exceed chemical accuracy, this requires adequately accounting for valence electron correlation, core electron correlation, zero-point vibrational energy (ZPVE), higher-order electron correlation (HOC), relativistic effects, and non-adiabatic effects through a Diagonal Born-Oppenheimer Correction (DBOC). These various terms are illustrated in Figure 1, which is a flowchart of the new procedure.

Throughout this work conventional and explicitly-correlated (F12) coupled cluster calculations were carried out. For the explicitly-correlated valence electron calculations the cc-pV*n*Z-F12 (*n*=T, Q, 5) basis sets were used, while the core-valence calculations were carried out with the cc-pCV*n*Z-F12(*n*=T, Q) family of basis sets.[26-28] For each basis, the default recommended auxiliary CABS, and RI basis sets developed for use with each of these sets were used respectively, along with the same geminal Slater exponent of 1.4 for the valence calculations and for the core-valence calculations.[19-21] The explicitly-correlated calculations used the F12b method of Werner and coworkers[29] along with the fixed amplitude 3C(FIX)[30] ansatz. The conventional coupled-cluster calculations were carried out using cc-pV*n*Z (*n*=D, T), aug-cc-pVTZ, and aug-cc-pCVTZ[31] basis sets. All CCSD(T)-F12b computations were performed with MOLPRO 2015[32] using gradient and energy convergence criteria tighter than default (10^{-5} and 10^{-10}, respectively). For open-shell species the ROHF/UCCSD(T)-F12b variant was used; the ROHF reference was used for the HOC term for consistency with the other calculations. HOC calculations beyond CCSD(T) were carried out using CCSDT and CCSDT(Q) with MRCC.[33,34] For open-shelled species, the *B* ansatz is specified for (Q).[35] VPT2 calculations were performed with the SURF code in MOLPRO.[36,37]

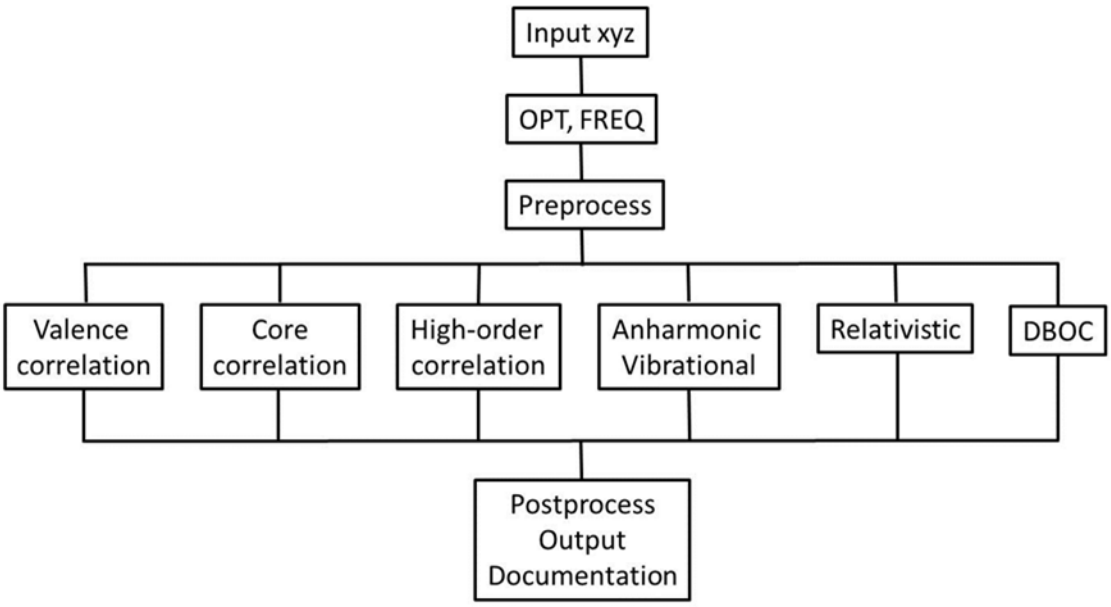

Figure 1: Flowchart of the automated thermochemical protocol. Details of each contribution to the composite energy and the pre- and post-processing procedures are given in the text.

Our newly developed composite thermochemistry approach is the following: 1) the molecular geometry is optimized with CCSD(T)-F12b/cc-pVTZ-F12, 2) the anharmonic ZPVE as well as fundamental vibrational levels are computed using VPT2[38] with resonances analyzed and removed at the CCSD(T)-F12b/cc-pVTZ-F12 level, 3) CCSD(T)-F12b/cc-pV*n*Z-F12 (*n*=T-5) are carried out to obtain the HF and valence correlation energies, 4) the core correlation contribution is defined as the energy difference between all electron and valence only CCSD(T)-F12b/cc-pCV*n*Z-F12(*n*=T, Q) calculations, 5) the HOC contribution is calculated as the sum of ΔT and ΔQ with ΔT=CCSDT-CCSD(T) using the cc-pVTZ basis set and ΔQ=CCSDT(Q)-CCSDT using the cc-pVDZ basis set, 6) the contribution of scalar relativistic effects is calculated as the expectation values of the mass-velocity and one-electron Darwin operators using CFOUR[39] at the CCSD(T)/aug-cc-pCVTZ level of theory, 6) DBOC is calculated using ROHF with the aug-cc-pVTZ basis set with CFOUR,[40] and 7) spin-orbit (SO) contributions are included for atomic spin-orbit coupling.[7] None of the molecular species considered here have first-order SO effects, so molecular SO effects were not considered.

The above protocol has been automated and gives the total energy as:

$$E = E_{HF} + E_{CCSD} + E_{(T)} + E_{Core} + E_{HOC} + E_{Rel} + E_{ZPVE} + E_{DBOC} + E_{SO} \quad (1).$$

The automated protocol, governed by Python scripts is flexible in its implementation and so results for a variety of different procedures can be compared. For *Procedure 1*, the core-correlation term and the HOC term both include only the largest employed single basis (without extrapolation), whereas for *Procedure 2*, each of those contributions is extrapolated. *Procedure 3* and *Procedure 4* are respectively similar to *Procedures 1* and *2* except that the structure and harmonic frequencies are obtained with the pVDZ-F12 basis set instead of pVTZ-F12, and some additive corrections are computed using computationally less demanding methods. CCSD(T)-F12b using the pVDZ-F12 basis set has previously been demonstrated to give good harmonic ZPVE's.[41] The two differences in additive corrections of *Procedure 3* and *Procedure 4* are the scalar relativistic correction and the VPT2 anharmonic correction. The scalar relativistic correction is carried out in MOLPRO using second order Douglas-Kroll instead of expectation values from CFOUR. Rather than use CCSD(T)-VPT2, the VPT2 correction is obtained with B3LYP and the cc-pVTZ basis set of Dunning and coworkers. The VPT2 procedure in Gaussian 09[42] is described by Barone.[43] B3LYP/cc-pVTZ has previously been demonstrated to yield satisfactory anharmonicity correction's to the ZPE relative to the harmonic ZPE, compared to reference results obtained by DMC on a CCSD(T)/cc-pVTZ surface.[48] *Procedure 4* is similar to *Procedure 2* except for the two changes described above. Uncertainty estimates for *Procedure 3* and *Procedure 4* are determined the same way as for *Procedure 1* and *Procedure 2*.

The automated procedure starts with an inputted approximate Cartesian structure and begins by performing an optimization and harmonic frequency calculation. In what is labeled *Preprocess* in the flowchart of Figure 1, the optimized geometry is recorded, and the harmonic frequencies are checked for imaginary or low-frequency modes (because large amplitude motion modes might introduce significant error into the anharmonic vibrational contribution). The T_1 diagnostic is also recorded as one possible indication of multireference character. Next, the optimized geometry is passed forward, and the six contributions to the total energy are computed separately using various different codes and resources, with allocations balanced by consideration of the relative cost, efficiency of parallelization etc. Once completed, the timing for each contribution is recorded, and, in order to confirm proper convergence, the value recorded for each term is examined to ensure that it is within a reasonable range. A few additional tests are made, including examining the relative contribution of HOC to the total atomization energy (another possible indication of multireference character), as well as looking for unusually large anharmonic

corrections to the vibrational frequencies. These steps correspond to the *Postprocessing* of Figure 1. All of this is done automatically using Python scripting, which also produces a master output summarizing the results (including the derived enthalpy of formation and atomization energy). More details about these tests and the general breadth of applicability of these procedures that has been determined will be given in a forthcoming article.

CBS extrapolations were carried out using three different formulas including the l^{-3} approach ($E_n^{corr} = E_{CBS}^{corr} + \frac{A}{l_{max}^3}$), employing the two largest basis set used in a given term. The uncertainty of extrapolation is estimated using the statistics of three different schemes: the l^{-3} approach,[44] a Schwenke extrapolation procedure,[45] and an l^{-4} extrapolation method.[46] The coefficients for the extrapolation using Schwenke's formula are those derived by Hill *et al*.[47] The Schwenke extrapolated (T) term was used in the composite energy. Our approach separated the CCSD and (T) terms to account for differences in the convergence behavior of CCSD vs. (T) energies due to explicit correlation of CCSD. A similar approach has been used by Feller to determine uncertainties in other highly accurate computed enthalpies of formation.[48,49]

Enthalpies of formation for 0 K and 298.15 K were determined by first computing the atomization energy of the molecule in question, and then determining the enthalpy of formation via the difference between the reference atomic enthalpies of formation and the atomization energy (the same approach was used in reference 7). To avoid introducing error due to the presence of a hindered rotor, the contribution of the lowest frequency mode was removed at 298.15 K. The enthalpies of formation for the atomic species were taken from reference 25, the current version of Active Thermochemical Tables.

Results and Discussion

The HF term has previously been shown to be well converged towards the CBS limit with the large basis set (cc-pV5Z-F12) employed in this work.[21] We also found that non-extrapolated CCSD-F12b with the cc-pV5Z-F12 basis paired with an extrapolation of the (T) term using the VTZ-F12 and VQZ-F12 basis sets and a Schwenke extrapolation,[45,47] yields well-converged results compared with higher cost benchmarks. For most of the other terms in the composite scheme, uncertainty contributions were determined as half the difference to the next larger possible basis computation. For the DBOC term, no uncertainty was assigned this way due to DBOC's

weak basis set dependence,[48] and while CCSD/DBOC is feasible with CFOUR, our tests found the differences to be negligible for these systems.

Table 1 summarizes the energy contributions for each species considered in this study. A version of ATcT TN denoted 1.122-q-pre was initially constructed from the previously existing thermochemical data mentioned in the introduction, and these, along with the results of several standard mid-level computations (such as W1, CBS-APNO, G3X, G4, CBS-QB3), were used to benchmark the composite protocol developed here. The thermochemical data for reactions involving methylperoxy included in this version of the TN are detailed in Table 2.[25] After inclusion of the new results, the resulting recommended enthalpies of formation from a version of ATcT TN denoted 1.122q, based on these reactions and the current work is given in Table 3. Table 4 compares the anharmonic vibrational frequencies computed with VPT2 with experimental assignments where available. Although experimental data is somewhat limited for these species (altogether only 13 fundamental frequencies), the level of agreement is impressive, instilling confidence in what can easily be a rather large source of overall error.[50] Not only is the root-mean-squared deviation (RMSD) low (5.61 and 2.51 cm^{-1} for CH_3O_2 radical and CH_3O_2H respectively), but the errors are distributed about the mean leading to some cancelation of error in the overall ZPVE contribution.

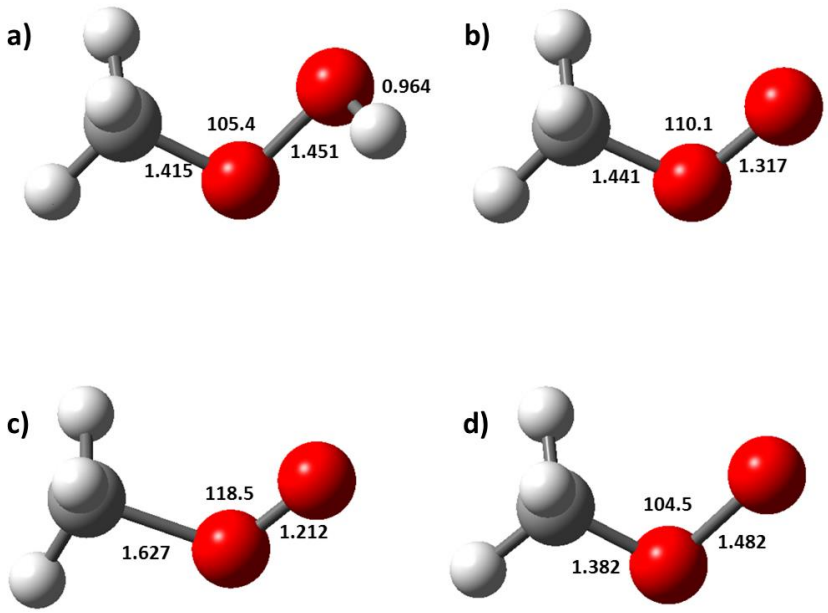

Figure 2: Some relevant structural parameters for members of the methylperoxy family (distances in Angstroms and angles in degrees). CH_3O_2 structures b), c) and d) are those of the neutral radical, cation, and anion systems, respectively.

A. Methylperoxy radical

The methylperoxy radical (doublet) has received significant attention in the literature due to its importance in atmospheric and combustion processes.[2,51-58] Table 2 summarizes available reaction thermochemistry for it. A provenance analysis[48,59] by variance decomposition of the enthalpy of formation of methylperoxy shows that the primary contributor to the in TN version 1.122q-pre is the HEAT345(Q) determination of Nguyen *et al*. for the dissociation of methylperoxy into methyl and oxygen,[60] and the enthalpy of CH_3 has previously been well established.[59] This theoretical determination accounts for 41% of the variance, and is consistent with a third-law analysis performed on the experimental data of Slagle and Gutman.[61] A third-law analysis of Knyazev and Slagle[62] yields a reaction enthalpy that is 2.3 kJ/mol above that reported by Slagle and Gutman and 4.3 kJ/mol above the HEAT345(Q) value, but the statistical analysis carried out by ATcT increases the reported 2.1 kJ/mol error bar by a factor of 1.8 because it is mutually inconsistent with the HEAT345(Q) determination, the earlier analysis of Slagle and Gutman, and two photoionization appearance energies of methylium from methylperoxy.[55,56] Second-law analyses by Slagle and Gutman and Knyazev and Slagle yield values that are consistent with all three values, but their uncertainties are so large that these reactions do not appreciably contribute to provenance. There is also a determination of the equilibrium constant of methylperoxy and methyl from Khachatryan *et al*. that is also consistent with these determinations.[63] There are other theoretical determinations included in the network that are also consistent, but the distributed provenance of methylperoxy across several consistent experimental determinations, in addition to the well-established enthalpy of formation of methyl and methylium gives confidence that the heat of formation of methylperoxy is well established in TN version 1.122q-pre. Our current computational results agree well with the HEAT-345(Q) results of Nguyen *et al*.,[60] the ANL0 results of Klippenstein *et al*.,[17] the CCSD(T) results of Shallcross *et al*.,[54] and the results of ATcT TN version 1.122q-pre. The results of the present calculations were added to the TN, resulting in ATcT TN version 1.122q, which unsurprisingly yields a similar enthalpy of

formation for methylperoxy to the prior version, albeit with a slightly smaller uncertainty due to the inclusion of more high accuracy composite thermochemistry of related species.

B. Methoxyoxoniumylidene (methylperoxy cation)

The structure of the (triplet) cation species is shown in Figure 2. Interestingly, the C-O bond is very long at 1.63 Å, while the O-O bond length is quite short (close to that of a free O_2 diatomic). Methoxyoxoniumylidene is the photoionization product of the methylperoxy radical,[55,56] and has been observed by mass spectrometry.[64] Interestingly the methylperoxy cation is the only known stable alkylperoxy cation (the larger ones have not been found to be stable).[56] The photoionization[56] and photoelectron[55] observations of methoxyoxoniumylidene from methyl peroxy, in combination with mid-level composite theory results (W1, CBS-APNO, G3X, G4, CBS-QB3) and the provenance of methylperoxy mentioned above yielded the majority of the provenance of CH_3OO^+. The resulting reaction enthalpies shown in Table 2 are in excellent agreement with the present results.

C. Methylhydroperoxide

Methylhydroperoxide has received a large amount of attention both experimentally and computationally due to its role in NO_2 production in the atmosphere.[65-71] The optimized structure obtained in this work is shown in Figure 2. The geometry of the heavy-atom backbone is similar to that of the CH_3O_2 anion discussed next. Matthews *et al*.[71] determined the onset of methoxy and hydroxyl from methylhydroperoxide via laser induced fluorescence and reported two values, one from the maximum OH excitation energy, and the other from the average.[71] These determinations are consistent with, but less accurate than the theoretical determination of the enthalpy in the same work, which is the dominant contributor to the provenance of the enthalpy of formation of CH_3OOH at 9%. Generally the provenance of CH_3OOH is well distributed including the above reactions, a photoelectron study,[72] and a variety of theoretical determinations.[17,73,74] The gas phase acidity of Blanksby *et al*.[75] is inconsistent with the remainder of the thermochemical network, and the ATcT statistical analysis increases their reported error bar by a factor of three. Our present computational results agree well with the CHEAT results of Faragó *et al.*,[73] the ANL0 results of Klippenstein *et al.*,[17] those of Simmie *et al.*,[74] and the results of ATcT TN version 1.122q-pre.

D. Methylperoxy anion

Table 3 summarizes the results for this singlet species. The structure is shown in Figure 2 and is most similar to that of the back-bone of methylhydroperoxide. Compared to the other members of the family studied in this work, this species has received comparably little attention. The initial ATcT TN version 1.122q-pre was constructed with the reactions shown in Table 2. The photoelectron results from Blanksby *et al*.[75] are consistent with mid-level composite theory results (W1, CBS-APNO, G3X, G4, CBS-QB3), and due to the small uncertainty of those results this determination alone accounts for 43% of the provenance of methylperoxy anion. The remaining provenance is primarily distributed over reactions that were described in the determination of the enthalpy of formation of methyl peroxide. Our current computational results agree well with Blanksby *et al*. and ATcT 1.122q-pre.

E. Ethylperoxy radical, ethylhydroperoxide, and ethylperoxy anion

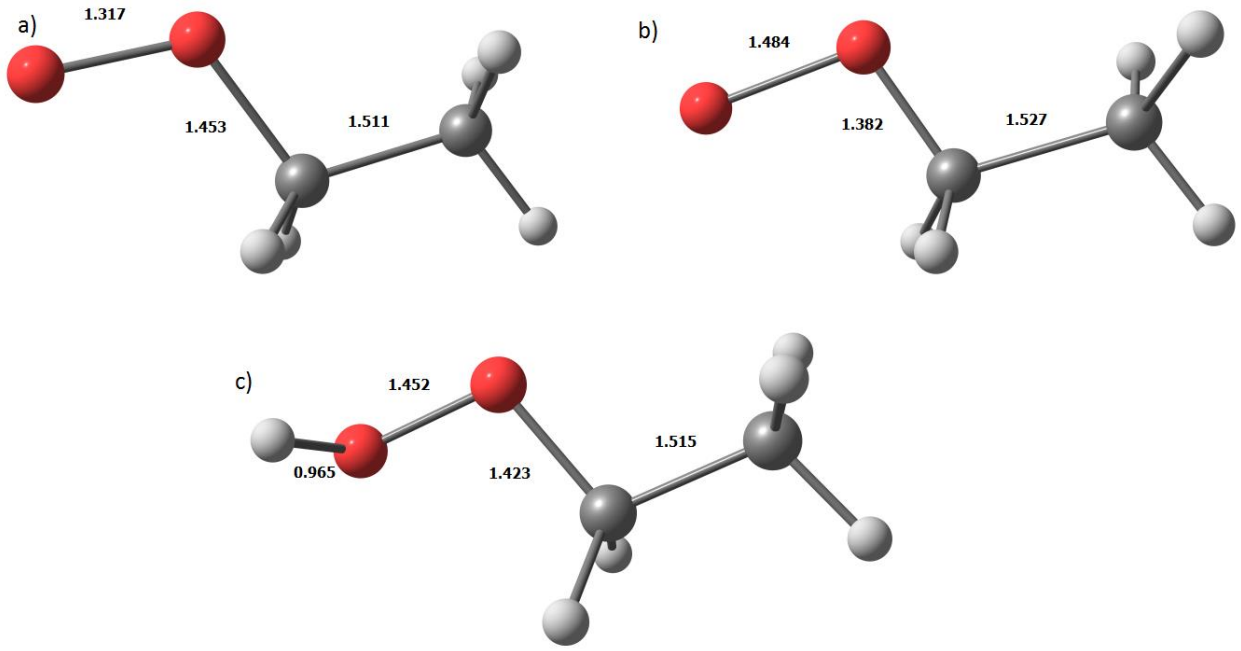

Figure 3: Some relevant structural parameters of the ethylperoxy and ethylhydroperoxide species; a) the radical, b) the anion, and c) the ethylhydroperoxide species.

Figure 3 shows the structure of the ethylperoxy radical as well as the related species calculated in this study. Using ATcT heats of formation for the atoms at 0 K, the heat of formation of ethylperoxy computed from the total atomization energy at 0 K for Procedures 3 and 4 are respectively -5.56 ± 2.19 and -4.73 ± 1.38 kJ mol^{-1}. These compare well with the work of

Klippenstein *et al.*,[17] -6.1 and -5.9 kJ mol^{-1} for ANO0 and ANO0-F12. This is unsurprising as both are high level computations based on CCSD(T) that systematically include HOC, DBOC, and calculated anharmonic corrections. The reduced uncertainties reported above are assigned from the additive errors estimated in both procedures and the above results for methylperoxy and related species. Procedure 4 has a slightly smaller uncertainty due to the basis set extrapolations carried out and had an RMSD of 2.0 kJ/mol comparable to ATcT's result for methyl peroxy and related species. Our work also agrees well with the 0 K obtained from the computational approach of ref. 58 (-5.00±3.77 kJ mol^{-1}).

Table 5 reports the enthalpy of formation for these 3 species at 0 K. The Procedure 3 and Procedure 4 0K enthalpy of formation of ethylhydroperoxide are -142.23±2.30 and -141.25±1.39 kJ mol^{-1}. These are in good agreement with the values of Klippenstein *et al.*[17] and the computationally less expensive approach of Goldsmith *et al.*[58] The negative-ion photoelectron spectra have been experimentally observed, with Blanksy *et al.*[75] obtaining an EA of 1.186 ± 0.004 eV.[44] This is slightly higher than the EAs of 1.170 eV and 1.167 eV obtained here from Procedure 3 and Procedure 4, respectively.

Conclusion

We present a flexible automated thermochemical computational protocol based on explicitly-correlated coupled-cluster theory designed to generate benchmark level enthalpies of formation and atomization energies for small to medium-sized molecular species. The workflow is governed by Python scripts and include flexible components of a newly derived composite energy scheme including valence, core, and high-order electron correlation, as well as anharmonic vibrational levels, and corrections for relativistic and non-Born-Oppenheimer effects. All of the codes are run automatically, including the post-processing of results, as well as convergence checks and gathering the necessary documentation of all input and output files.

The procedure was demonstrated on the smallest family of alkyl peroxide and hydroperoxide species, the methyl family. Enthalpies of formation were calculated at 0 K and 298.15 K and compared with other calculations, experiments, and the existing ATcT network. The new values are consistent with the current ATcT database. Conservative uncertainties are assigned to the calculated data as part of the procedure and these were found to overlap with those of the

existing network. The agreement between the data for the methylperoxy species gives confidence to the predictions made for ethylperoxy species.

This new validated automated procedure is a convenient way for the ATcT network to expand in a community driven way as the workflow can be applied to a variety of species of interest, and the results so obtained can be interfaced to update the network.

Acknowledgement

The work at Argonne National Laboratory was supported by the U.S. Department of Energy, Office of Science, Office of Basic Energy Sciences, Division of Chemical Sciences, Geosciences and Biosciences, under Contract No. DE-AC02-06CH11357, through the Gas-Phase Chemical Physics Program (BR) and the Computational Chemical Sciences Program (DHB). This research used resources of the Argonne Leadership Computing Facility, which is a DOE Office of Science User Facility supported under Contract DE-AC02-06CH11357. We gratefully acknowledge computing resources provided by Bebop, a high-performance computing cluster operated by the Laboratory Computing Resource Center at Argonne National Laboratory. B.W. and R.D. are supported by the U.S. Department of Energy, Office of Science, Office of Basic Energy Sciences, Grant no. DE-SC0019740.

Table 1: Electronic Energies of Atoms and Molecules

Procedure 1[a]									
Species	ΔE(HF)	ΔE(CCSD)	ΔE(T)	ΔE(Core)	ΔE(ZPVE)	ΔE(DBOC)	ΔE(Rel+SO)	ΔE(HOC)	Total
C	-37.688688	-0.097907	-0.002669	-0.054632	0.000000	0.001660	-0.015141	-0.000483	-37.857862
O	-74.812384	-0.187840	-0.004287	-0.061573	0.000000	0.002366	-0.052692	-0.000356	-75.116767
H	-0.499999	0.000000	0.000000	0.000000	0.000000	0.000272	-0.000007	0.000000	-0.499734
CH_3OO	-189.288871	-0.717198	-0.030443	-0.179842	0.042552	0.007081	-0.119062	-0.002226	-190.288009
$[CH_3OO]^+$	-188.943335	-0.684979	-0.029641	-0.179303	0.041398	0.007083	-0.119284	-0.002853	-189.910950
$[CH_3OO]^-$	-189.278712	-0.763876	-0.035445	-0.179740	0.040701	0.007130	-0.118909	-0.001876	-190.330727
CH_3OOH	-189.895143	-0.756237	-0.031559	-0.179998	0.054028	0.007248	-0.118909	-0.001843	-190.922455
Procedure 2[a]									
C	-37.688688	-0.097907	-0.002669	-0.054814	0.000000	0.001660	-0.015141	-0.000545	-37.858107
H	-0.499999	0.000000	0.000000	0.000000	0.000000	0.000272	-0.000007	0.000000	-0.499734
O	-74.812384	-0.187840	-0.004287	-0.062088	0.000000	0.002366	-0.000671	-0.000427	-75.117353
CH_3OO	-189.288871	-0.717198	-0.030443	-0.181137	0.042552	0.007081	-0.119062	-0.002109	-190.289188
$[CH_3OO]^+$	-188.943335	-0.684979	-0.029641	-0.180589	0.041364	0.007083	-0.119284	-0.002810	-189.912192
$[CH_3OO]^-$	-189.278711	-0.763876	-0.035444	-0.181020	0.040701	0.007130	-0.118909	-0.001668	-190.331799
CH_3OOH	-189.895143	-0.756237	-0.031559	-0.181286	0.054028	0.007248	-0.118909	-0.001669	-190.923568
Procedure 3									
C	-37.688688	-0.097907	-0.002669	-0.054632	0.000000	0.001660	-0.015141	-0.000483	-37.857862
O	-74.812384	-0.187840	-0.004287	-0.061573	0.000000	0.002366	-0.052692	-0.000356	-75.116767
H	-0.499999	0.000000	0.000000	0.000000	0.000000	0.000272	-0.000007	0.000000	-0.499734
CH_3OO	-189.288818	-0.717228	-0.030461	-0.179838	0.042617	0.007080	-0.119062	-0.002232	-190.287944
$[CH_3OO]^+$	-188.943340	-0.684971	-0.029642	-0.179305	0.041501	0.007082	-0.119284	-0.002668	-189.910629
$[CH_3OO]^-$	-189.278675	-0.763896	-0.035458	-0.179738	0.040735	0.007130	-0.118909	-0.001876	-190.330689
CH_3OOH	-189.895047	-0.756310	-0.031621	-0.179997	0.054155	0.007248	-0.118910	-0.001846	-190.922326
CH_3CH_2OO	-228.345178	-0.914513	-0.039035	-0.236353	0.070831	0.009187	-0.1337738	-0.002575	-229.591411
$[CH_3CH_2OO]^-$	-228.335049	-0.961058	-0.044134	-0.236229	0.068662	0.009238	-0.133621	-0.002222	-229.634413
CH3CH2OOH	-228.950969	-0.95365902	-0.040255	-0.236495	0.082385	0.009355	-0.1336231	-0.002221	-230.225483
Procedure 4									
C	-37.688688	-0.097907	-0.002669	-0.054814	0.000000	0.001660	-0.015141	-0.000545	-37.858107
O	-74.812384	-0.187840	-0.004287	-0.062088	0.000000	0.002366	-0.000671	-0.000427	-75.117353
H	-0.499999	0.000000	0.000000	0.000000	0.000000	0.000272	-0.000007	0.000000	-0.499734
CH_3OO	-189.288818	-0.717228	-0.0303928	-0.181125	0.042617	0.007080	-0.119062	-0.002115	-190.289114
$[CH_3OO]^+$	-188.943340	-0.684971	-0.029578	-0.180583	0.041501	0.007082	-0.119284	-0.002546	-189.911785
$[CH_3OO]^-$	-189.278675	-0.763896	-0.029642	-0.181012	0.040735	0.007130	-0.118909	-0.001668	-190.331755
CH_3OOH	-189.895047	-0.756310	-0.031551	-0.181278	0.054155	0.007248	-0.118910	-0.001672	-190.923433
CH_3CH_2OO	-228.345178	-0.914513	-0.039035	-0.237857	0.070831	0.009187	-0.133773	-0.004367	-229.592759
$[CH_3CH_2OO]^-$	-228.335049	-0.961058	-0.044134	-0.237721	0.068662	0.009238	-0.133621	-0.001975	-229.635658
CH3CH2OOH	-228.950969	-0.95365902	-0.040255	-0.237993	0.082385	0.009355	-0.133623	-0.002012	-230.226772

[a] *Procedures 1-4* are described in the text. *Procedure 2 and 4* involve additional CBS extrapolation.

Table 2: Comparison of present results to previously reported thermochemistry data

Reaction	Determination	Value	ΔH(0K) kJ/mol[a]	ΔH(0K) kJ/mol Present work[b]	Reference
$CH_3OOH_{(g)} \rightarrow [CH_3OOH]_{(g)}^+$	Photoelectron	ΔH(0K)= 9.87±0.05 eV	952.3±4.8	948.8	72
$CH_3OO_{(g)} \rightarrow [CH_3OO]_{(g)}^+$	Photoelectron	ΔH(0K)=10.265±0.025 eV	990.5±2.4	991.8	55
	Photoionization	ΔH(0K)= 10.33±0.05 eV	996.7±4.8		56
	Theory CBS-APNO	ΔH(0K)=10.21eV	985.1		56
$[CH_3OO]_{(g)}^- \rightarrow CH_3OO_{(g)}$	Photoelectron	ΔH(0K)= 1.161±0.005 eV	112.02±0.48	112.99	75
$CH_3OO_{(g)} \rightarrow [CH_3]^+_{(g)} + O_{2(g)}$	Photoionization	ΔH(0K)= 11.16±0.05 eV	1076.8±4.8	1077.4	56
	Photoionization	ΔH(0K)= 11.164±0.01 eV	1077.2±1.0		55
$CH_3OO_{(g)} \rightarrow CH_{3(g)} + O_{2(g)}$	Radical freezing	ΔG(750K)= 8.49±3.44 kcal/mol	129±14	128.0	63
	3rd law gas phase equilibrium	ΔG(753K)= 8.55±0.38 kcal/mol	129.2± 1.6		61
	2nd law gas phase equilibrium	ΔH(753K)= 31.9±2.9 kcal/mol	125±12		61
	3rd law gas phase equilibrium	ΔG(753K)= 9.09±0.51 kcal/mol	131.5±2.1		62
	2nd law gas phase equilibrium	ΔH(753K)= 33.8±3.8 kcal/mol	133±16		62
	Theory HEAT345(Q)	ΔH(0K)=30.4 kcal/mol	127.2		60
	Theory mHEAT345(Q)	ΔH(0K)=30.75 kcal/mol	128.7		60
$CH_3OO_{(g)} + 5/2\ H_{2(g)} \rightarrow CH_{4(g)} + 2H_2O_{(g)}$	Theory	ΔH(0K)= -135.86 kcal/mol	-568.4	-566.3	54
$[CH_3OO]_{(g)}^- + HCCH_{(g)} \rightarrow [CCH]_{(g)}^- + CH_3OOH_{(g)}$	Gas Phase Acidity	ΔG(298.15K)= 2.7 ±0.6 kcal/mol	16.0±2.5	24.2	75
$CH_3OO_{(g)} \rightarrow C_{(g)} + 3H_{(g)} + 2O_{(g)}$	Theory HEAT345(Q)	ΔH(0K)= 1831.0 kJ/mol	1831.0	1831.3	60
	Theory ANL0	ΔH(0K)= 1831.3 kJ/mol	1831.3		17
	Theory ANL0-F12	ΔH(0K)= 1833.1 kJ/mol	1833.1		17
$CH_3OOH_{(g)} \rightarrow C_{(g)} + 4H_{(g)} + 2O_{(g)}$	Theory ANL0	ΔH(0K)= 2184.8 kJ/mol	2184.8	2184.6	17
	Theory ANL0-F12	ΔH(0K)= 2186.7 kJ/mol	2186.7		17
$BrO_{(g)} + CH3OO_{(g)} \rightarrow HOBr_{(g)} + CH2OO_{(g)}$	Theory	ΔH(0K)= -22.48 kcal/mol	-94.1	-92.7	54
$CH_3OOH_{(g)} \rightarrow CH_3O_{(g)} + OH_{(g)}$	Laser Induced Fluorescence	ΔH(0K)= 14775 cm^{-1}	176.7	181.4	71
	Laser Induced Fluorescence	ΔH(0K)= 15070 cm^{-1}	180.3		71

$CH_3OOH_{(g)} \rightarrow CH_{3(g)} + HO_{2(g)}$	Theory CHEAT1	ΔH(0K)= 66.9±0.7 kcal/mol	279.9	280.4	73

[a]0 K values for finite temperature experiments derived from partition functions in ATcT version 1.122q-pre.

[b]For reactions containing species not currently calculated the reaction enthalpy has been included from ATcT version 1.122q-pre and the current composite thermochemistry results from *Procedure 1*.

Table 3: Recommended Enthalpies of Formation from ATcT TN 1.122q kJ/mol

Species Name	Formula	ΔH_f (0K)	ΔH_f(298.15K)	Uncertainty
Methylperoxy	$CH3OO_{(g)}$	22.05	12.60	± 0.36
Methoxyoxoniumylidene	$CH3OO^{+}_{(g)}$	1013.65	1004.82	± 0.67
Methylperoxy anion	$CH3OO^{-}_{(g)}$	-90.38	-100.52	± 0.48
Methylhydroperoxide	$CH3OOH_{(g)}$	-115.16	-127.99	± 0.49

Table 4: Comparison of vibrational frequencies (cm^{-1}) calculated at the VPT2 CCSD(T)-F12b/cc-pVTZ-F12 level with experiment.

CH_3O_2 radical[76,77]		CH_3O_2H[78]		CH_3O_2 anion	CH_3O_2 cation
Calc.	Expt.	Calc.	Expt.	Calc.	
3029.25	3030.0	3600.47	x	2818.35	3109.46
3015.80	3020.0	2997.23	x	2779.38	3089.47
2962.00	2968.0	2967.92	2963.8	2700.93	2969.77
1454.35	1453.0	2906.39	x	1460.08	1482.41
1440.12	1440.0	1479.21	1478.1	1390.82	1401.45
1416.87	1414.0	1432.94	x	1381.09	1391.24
1185.87	1183.0	1421.07	x	1177.00	1352.88
1135.13	x	1321.56	1320.7	1143.15	1042.57
1120.39	1112.0	1179.50	x	1064.08	1002.11
915.12	902.0	1155.42	x	777.72	463.91
492.02	492.0	1026.25	x	425.33	308.76
136.19	x	831.07	x	264.6	104.33
5.61	**RMSD**	443.97	x		
		243.82	x		
		176.76	x		
		2.51	**RMSD**		

No known experimental data assigned for the anion and cation species

Table 5: Enthalpy of formation (kJ/mol) of ethylperoxy and related species

Molecule	Determination	Type	Enthalpy	T(K)	Ref
CH_3CH_2OO	Knyazev and Slagle	Experiment	-27.19±10.14	298.15	62
	Goldsmith *et. al.*	QCI Method	-5.00±3.77	0	58
		QCI Method	-20.92±3.77	298.15	
	Blanksby *et al.*	CBS/APNO	-28.45±2.93	298.15	75
		Combination	-28.45±9.62		
	Bozzelli and Wang	Average of theories	-25.90±3.85	298.15	69
	Klippenstein *et al.*	ANL0	-6.1	0	17
		ANL0-F12	-5.9	0	
	Present work	Procedure 3	-5.56±2.19	0	
			-27.27±2.19	298.15	
		Procedure 4	-4.73±1.38	0	
			-26.45±1.38	298.15	
CH_3CH_2OOH	Stathis and Egerton	Experiment	-188.28±50.21	298.15	79
	Goldsmith *et. al.*	QCI Method	-142.80±3.77	0	58
		QCI Method	-161.08±3.77	298.15	
	Blanksby et al.	CBS/APNO	-165.27±2.93	298.15	75
	Bozzelli and Wang	Average of theories	-162.92±3.39	298.15	69
	Klippenstein *et al.*	ANL0	-141.1	0	17
		ANL0-F12	-140	0	
	Present work	Procedure 3	-142.23±2.30	0	
			-167.09±2.30	298.15	
		Procedure 4	-141.25±1.39	0	
			-166.13±1.39	298.15	
$[CH_3CH_2OO]^-$	Blanksby et al.	Experiment	-114.432±0.386	0	75
		Combination	-142.88±9.63	298.15	
	Present Work	Procedure 3	-118.46±2.67	0	
			-139.96±2.67	298.15	
		Procedure 4	-117.36±1.70	0	
			-138.86±1.70	298	

REFERENCES

[1] Müller, J.-F. C. A.; Liu, Z.; Nguyen, V. S.; Stavrakou, T.; Harvey, J. N.; Peeters, J. The reaction of methyl peroxy and hydroxyl radicals as a major source of atmospheric methanol. *Nature Communications* **2016**, *7*, 13213.

[2] Launder, A. M.; Agarwal, J.; Schaefer, H. F. Exploring Mechanisms of a Tropospheric Archetype: CH_3O_2 + NO. *J. Chem. Phys*. **2015**, *143*, 234302/1-234302/10.

[3] Nguyen, L.T; McCarthy, C.M; Stanton, F,J. Relatively Selective Production of the Simplest Criegee Intermediate in a CH_4/O_2 Electric Discharge: Kinetic Analysis of a Plausible Mechanism. *J.Phys.Chem.A.* **2015**, 28, 7197-7204.

[4] Sullivan, N. E.; N, Bethan, N. M. Photodissociation dynamics of the simplest alkyl peroxy radicals, CH_3OO and C_2H_5OO, at 248 nm. *J. Chem. Phys.* **2018**, 148, 044309/1-044309/12.

[5] Lightfoot, P. D.; Cox, R. A.; Crowley, J. N.; Destriau, M.; Hayman, G. D.; Jenkin, M. E.; Moortgat, G. K.; Zabel F. Organic peroxy radicals: Kinetics, spectroscopy and tropospheric chemistry**.** *Atmos. Environ. A* **1992**, 26, 1805-1961.

[6] Tyndall, G. S.; Cox, R. A.; Granier C.; Lesclaux, G. K.; Moortgat G. K.; Pilling, M. J.; Ravishankara, A. R.; Wallington, T. J. Atmospheric chemistry of small organic peroxy radicals. *J. Geophys. Res.* **2001**, 26, 12157-12182.

[7] Tajti, A.; Szalay, P. G.; Császár, A. G.; Kállay, M.; Gauss, J.; Valeev, E. F.; Flowers, B. A.; Vázquez, J.; Stanton, J. F. HEAT: High accuracy extrapolated ab initio thermochemistry. *J. Chem. Phys.* **2004**, *121*, 11599–11613.

[8] Harding, M. E.; Vázquez, J.; Ruscic, B.; Wilson, A. K.; Gauss, J.; Stanton, J. F. High-Accuracy extrapolated ab initio thermochemistry. III. Additional improvements and overview. *J. Chem. Phys.* **2008**, *128*, 114111/1-114111/15.

[9] Karton, A.; Rabinovich, E.; Martin, J. M. L.; Ruscic, B. W4 theory for computational thermochemistry: In pursuit of confident sub-kJ/mol predictions. *J. Chem. Phys.* **2006**, *125*, 144108/1-144108/17.

[10] Peterson, K. A.; Feller, D.; Dixon, D. A. Chemical accuracy in ab initio thermochemistry and spectroscopy: Current strategies and future challenges. *Theor. Chem. Acc*. **2012**, 131, 1079−1099.

[11] Ruscic, B. Uncertainty quantification in thermochemistry, benchmarking electronic structure computations, and Active Thermochemical Tables. *Int. J. Quantum Chem.* **2014**, 114, 1097–1101.

[12] Kállay, M.; Gauss, J. Approximate treatment of higher excitations in coupled-Cluster theory. II. Extension to general single-Determinant reference functions and improved approaches for the canonical Hartree–Fock case. *J. Chem. Phys.* **2008**, *129*, 144101/1-144101/9.

[13] Harding, M. E.; Vázquez, J.; Gauss, J.; Stanton, J. F.; Kállay, M. Towards highly accurate ab initio thermochemistry of larger systems: Benzene. *J. Chem. Phys.* **2011**, *135*, 044513/1-044513/10.

[14] Karton, A.; Sylvetsky, N.; Martin, J. M. L. W4-17: A Diverse and High-Confidence Dataset of Atomization Energies for Benchmarking High-Level Electronic Structure Methods. *J. Computat. Chem.* **2017**, *38*, 2063-2075.

[15] Ganyecz, C. C. A.; Kállay, M.; Csontos, J. Moderate-Cost Ab Initio Thermochemistry with Chemical Accuracy. *J. Chem. Theory Comput.* **2017**, *13*, 4193–4204.

[16] Chan, B.; Radom, L. W3X: A Cost-Effective Post-CCSD(T) Composite Procedure. *J. Chem. Theory Comput.* **2013**, *9*, 4769− 4778.
[17] Klippenstein, S. J.; Harding, L. B.; Ruscic, B. Ab Initio Computations and Active Thermochemical Tables Hand in Hand: Heats of Formation of Core Combustion Species. *J. Phys. Chem. A* **2017**, *121*, 6580–6602.
[18] Chan, B.; Radom, L. W2X and W3X-L: Cost-Effective Approximations to W2 and W4 with kJ mol–1 Accuracy. *J. Chem. Theory Comput* **2015**, *11*, 2109–2119.
[19] Thorpe, J. H.; Lopez, C. A.; Nguyen, T. L.; Baraban, J. H.; Bross, D. H.; Ruscic, B.; Stanton, J. F. High-Accuracy Extrapolated ab Initio Thermochemistry. IV. A Modified Recipe for Computational Efficiency. *J. Chem. Phys.* **2019**, submitted
[20] Karton, A.; Martin, J. M. L. Explicitly correlated Wn theory: W1-F12 and W2-F12. *J.Chem.Phys.***2012**, *136*, 124114/1-124114/12.
[21] Sylvetsky, N.; Peterson, K. A.; Karton, A.; Martin, J. M. L. Toward a W4-F12 approach: Can explicitly correlated and orbital-Based ab initio CCSD(T) limits be reconciled? *J. Chem. Phys* **2016**, *144*, 214101/1-214101/13.
[22] Chase, M. W., Jr.; Davies, C. A.; Downey, J. R., Jr.; Frirup, D. J.; McDonald, R. A.; Syverud, A. N. *NIST-JANAF Thermochemical Tables, 4th edition, J. Phys. Chem. Ref. Data Monogr.* **1998**, 9.
[23] Ruscic, B.; Pinzon, R. E.; Morton, M. L.; Laszevski, G. V.; Bittner, S. J.; Nijsure, S. G.; Amin, K. A.; Minkoff, M.; Wagner, A. F. Introduction to Active Thermochemical Tables: Several "Key" Enthalpies of Formation Revisited. *J. Phys. Chem. A* **2004**, *108*, 9979–9997.
[24] Ruscic, B.; Pinzon, R. E.; von Laszewski, G.; Kodeboyina, D.; Burcat, A.; Leahy, D.; Montoya, D.; Wagner, A. F. Active Thermochemical Tables: Thermochemistry for the 21st Century. *J. Phys. Conf. Ser.* **2005**, *16*, 561−570.
[25] Ruscic, B.; Bross, D. H. Active Thermochemical Tables (ATcT) Values Based on Ver. 1.122 of the Thermochemical Network, 2016; available at https://ATcT.anl.gov/
[26] Peterson, K. A.; Adler, T. B.; Werner, H.-J. Systematically convergent basis sets for explicitly correlated wavefunctions: The atoms H, He, B–Ne, and Al–Ar. *J. Chem. Phys.* **2008**, *128*, 084102/1-084102/12.
[27] Hill, J. G.; Mazumder, S.; Peterson, K. A. Correlation consistent basis sets for molecular core-Valence effects with explicitly correlated wave functions: The atoms B–Ne and Al–Ar. *J. Chem. Phys.* **2010**, *132*, 054108/1-054108/12.
[28] Peterson, K. A.; Kesharwani, M. K.; Martin, J. M. The cc-pV5Z-F12 basis set: reaching the basis set limit in explicitly correlated calculations. *Molecular Physics* **2014**, *113*, 1551–1558.
[29] Adler, T. B.; Knizia, G.; Werner, H.-J. A Simple and efficient CCSD(T)-F12 approximation. *J. Chem. Phys.* **2007**, 127, 221106/1-221106/4.
[30] Werner, H.-J.; Adler, T. B.; Manby, F. R. General orbital invariant MP2-F12 theory. *J. Chem. Phys.* **2007**, 126, 164102/1-164102/18.
[31] Woon, D. E., Dunning T. H. Jr.; Gaussian Basis sets for use in correlated molecular calculations. V. Core-valence basis sets for boron through neon. *J. Chem. Phys.* **1995**, 103, 4572-4585.
[32] Werner, H.-J.; Knowles, P. J.; Knizia, G.; Manby, F. R.; Schutz, M.; Celani, P.; Korona, T.; Lindh, R.; Mitrushenkov, A.; Rauhut, G.; et al. *MOLPRO*, version 2015.1, A Package of Ab Initio Programs; see http://www.molpro.net.
[33] Kallay, M.; Gauss, J. Approximate Treatment of Higher´ Excitations in Coupled-Cluster Theory. *J. Chem. Phys.* 2005, 123, 214105.

[34] Kallay, M. MRCC, A String-Based Quantum Chemical Program Suite
[35] Kállay, M. C. A.; Gauss, J. Approximate treatment of higher excitations in coupled-Cluster theory. II. Extension to general single-Determinant reference functions and improved approaches for the canonical Hartree–Fock case. *J. Chem. Phys.* **2008**, *129*(14), 144101/1-144101/9.
[36] Rauhut, G. Efficient Calculation of Potential Energy Surfaces for the Generation of Vibrational Wave Functions. *J. Chem. Phys.* **2004**, *121*, 9313-9322.
[37] Hrenar, T.; Werner, J, H.; Rauhut, G. Accurate Calculation of Anharmonic Vibrational Frequencies of Medium Sized Molecules Using Local Coupled Cluster Methods. *J. Chem. Phys.* **2007,** *126*, 134108/1-134108/9.
[38] Ramakrishnan, R.; Rauhut, G. Semi-Quartic Force Fields Retrieved from Multi-Mode Expansions: Accuracy, Scaling Behavior, and Approximations. *J. Chem. Phys*. **2015**, *142*, 154118/1-154118/8.
[39] Stanton, J. F.; Gauss, J.; Harding, M. E.; Szalay, P. G., with contributions from Auer, A. A.; Bartlett, R. J.; Benedikt, U.; Berger, C.; Bernholdt, D. E.; Bomble, Y. J.; et al., and the integral packages *MOLECULE* (Almlöf, J.; Taylor, P. R.), PROPS (Taylor, P. R.), *ABACUS* (Helgaker, T.; Jensen, H. J.; Jørgensen, P.; Olsen, J.), and ECP routines by Mitin, A. V.; van Wüllen, C. For the current version, see: http://www.cfour.de.
[40] Valeev, F, E.; Sherrill, D, C. The diagonal Born-Oppenheimer correction beyond the Hartree-Fock approximation *J. Chem. Phys.* **2003**, *118*, 3921-3927.
[41] Pfeiffer, F.; Rauhut, G.; Feller, D.; Peterson, K, A. Anharmonic zero point vibrational energies: Tipping the scales in accurate thermochemistry calculations. *J. Chem. Phys.* **2013**, *138*, 044311/1-044311/10.
[42] Frisch, M. J.; Trucks, G. W.; Schlegel, H. B.; Scuseria, G. E.; Robb, M. A.; Cheeseman, J. R.; Scalmani, G.; Barone, V.; Mennucci, B.; Petersson, G. A. *et al*. Gaussian 09, revision E.01; Gaussian, Inc.: Wallingford, CT, 2010.
[43] Barone, V. Anharmonic vibrational properties by a fully automated second-order perburbative approach *J. Chem. Phys.* **2005**, *122*, 014108/1-014108/10.
[44] Helgaker, T.; Klopper, W. Basis-set convergence of correlated calculations on water *J. Chem. Phys*. **1997**, *106*, 9639-9646.
[45] Schwenke, W, D. On one-electron basis set extrapolation of atomic and molecular correlation energies *Mol Phys*. **2012**, *110*, 2557-2567.
[46] Martin, J.M.L. Ab initio total atomization energies of small molecules –towards the basis set limit *Chem. Phys. Letters*. **1996**, *259*, 669-678.
[47] Hill, J, G.; Peterson, K, A.; G, Knizia, G.; Werner, H, J. Extrapolating MP2 and CCSD explicitly correlated correlation energies to the complete basis set limit with first and second row correlation consistent basis sets. *J. Chem. Phys.* **2009**, *131*, 194105/1-194105/13.
[48] Feller, D.; Bross, H, D.; Ruscic, B. Enthalpy of Formation of N_2H_4(Hydrazine) Revisited. *J. Phys. Chem. A*, **2017**, *121*, 6187-6198.
[49] Feller, D. Estimating the intrinsic limit of the Feller-Peterson-Dixon composite approach when applied to adiabatic ionization potentials in atoms and small molecules. *J. Chem. Phys.*,**2017**, *147*, 034103/1-034103/18.
[50] Karton, A.; Ruscic, B.; Martin, J. M. L. Benchmark Atomization Energy of Ethane: Importance of Accurate Zero-Point Vibrational Energies and Diagonal Born−Oppenheimer Corrections for a 'Simple' Organic Molecule. *J. Mol. Struct.: THEOCHEM* **2007**, *811*, 345−353.
[51] Yan, C.; Kocevska, S.; Krasnoperov, N, L. Kinetics of the Reaction of CH_3O_2 Radicals with OH Studied over the 292–526 K Temperature Range. *J. Phys. Chem. A*, **2016**, *120*, 6111-6121.

[52] Drougas,E Quantum mechanical studies of the CH_3O_2 + HO_2 reaction. *Comp and Theo Chem*, **2016**, *1093*, 98-103.
[53] Assaf, E.; Sheps, L.; Whalley, L.; Heard, D.; Tomas, A.; Schoemaecker, C.; Fittschen, C. The Reaction between CH_3O_2 and OH Radicals: Product Yields and Atmospheric Implications. *Environ. Sci. Technol*. **2017**, *51*, 2170−2177.
[54] Shallcross, D. E.; Leather, K. E.; Bacak, A.; Xiao, P.; Lee, E. P. F.; Ng, M.; Mok, D. K. W.; Dyke, J. M.; Hossaini, R.; Chipperfield, M. P.; Khan, M. A. H.; Percival Reaction between CH_3O_2 and BrO radicals: A new source of upper troposphere lower stratosphere hydroxyl radicals. *J. Phys. Chem. A* **2015**, *119*, 4618−4632.
[55]Voronva, K.; Ervin, K.; Torma, G, K.; Hemberger,.; Bodi, A.; Gerber, T.; Osborn, L, D.; Sztaray, B. Radical Thermometers, Thermochemistry, and Photoelectron Spectra: A Photoelectron Photoion Coincidence Spectroscopy Study of the Methyl Peroxy Radical. *J. Phys. Chem. Letters*. **2018**, *9*, 534-539.
[56] Meloni, G.; Zou, P.; Klippenstein, J, S.; Ahmed, M.; Leone, R, S.; Taatjes, A, C.; Osborn, D. Energy-Resolved Photoionization of Alkylperoxy Radicals and the Stability of Their Cations *J. Am. Chem. Soc*. **2006**, *128*, 13559-13567.
[57] Osborn, D. L. Reaction Mechanisms on Multiwell Potential Energy Surfaces in Combustion (and Atmospheric) Chemistry. *Annu. Rev. Phys. Chem*. **2017**, 68, 233−260.
[58] Goldsmith, C, F.; Magoon, R, G; Green, H, W. Database of Small Molecule Thermochemistry for Combustion. *J. Phys. Chem. A* **2012**, 36, 9033-9057.
[59] Ruscic, B.; Active Thermochemical Tables: Sequential Bond Dissociation Enthalpies of Methane, Ethane, and Methanol and the Related Thermochemistry. *J. Phys. Chem. A* **2015,** *119*, 7810-7837.
[60] Nguyen, L. T; McCarthy, C. M; Stanton, F, J.; Relatively Selective Production of the Simplest Criegee Intermediate in a CH_4/O_2 Electric Discharge: Kinetic Analysis of a Plausible Mechanism. *J. Phys. Chem. A.* **2015**, 28, 7197-7204.
[61] Slagle, I. R.; Gutman, D. J.; Kinetics of Polyatomic Free Radicals Produced by Laser Photolysis. 5. Study of the Equilibrium CH_3 + O_2 = CH_3O_2 between 421 and 538°C. *J. Am. Chem. Soc.* **1985**, 107, 5342-5347.
[62] Knyazev, V. D; Slagle, I. R; Thermochemistry of the R-O_2 Bond in Alkyl and Chloroalkyl Peroxy Radicals. *J. Phys. Chem. A* **1998**, 102, 1770-1778.
[63] Khachatryan, L. A.; Niazyan, O. M.; Mantashyan, A. A.; Vedeneev, V. I.; Teitel'boim, M. A.; Experimental Determination of the Equilibrium Constant of the Reaction CH_3 + O_2 = CH_3O_2 during the Gas-Phase Oxidation of Methane. *Int. J. Chem. Kinet.* **1982**, 14, 1231-1241.
[64] Schalley, C. A.; Schroeder, D.;Schwarz, H.; A neutralization-reionization mass spectrometric study of alkyl hydroperoxide cation radicals and four distinguishable [C,H3,O2]+ isomers. *International Journal of Mass Spectrometry and Ion Processes.* **1996**, 153, 173-199.
[65] Anglada, M, J.; Crehuet, R.; Costa-Martins, M.; Francisco, S, J.; Ruiz-Lopez, M.; The atmospheric oxidation of CH_3OOH by the OH radical: the effect of water vapor. *Phys. Chem. Chem. Phys*. **2017**, 19, 12331-12342.
[66] Harding, B, L.; Georgievskii, Y.; Klippenstein, J, S. Accurate Anharmonic Zero-Point Energies for Some Combustion-Related Species from Diffusion Monte Carlo. *J. Phys. Chem. A.* **2017**, 121, 4334-4340.
[67] Watanabe, K.; Yachi, C.; Song, J, X.; Kakuyama, S.; Nishibe, M.; Jin, J, S. Atmospheric hydroperoxides measured over a rural site in central Japan during spring: helicopter-borne measurements. *J. Atmos Chem.* **2017**, https://doi.org/10.1007/s10874-017-9368-6.

[68] Zhang, X.; He, Z, S.; Chen, M, Z.; Zhao, Y.; Hua, W. Methyl hydroperoxide (CH3OOH) in urban, suburban and rural atmosphere: ambient concentration, budget, and contribution to the atmospheric oxidizing capacity. *Atmos. Chem. Phys.* **2012**, 12, 8951-8962.
[69] Bozzelli, W, J.; Wang, H. Thermochemical Properties ($\Delta_f H°$(298 K), $S°$(298 K), $C_p(T)$) and Bond Dissociation Energies for C1–C4 Normal Hydroperoxides and Peroxy Radicals. *J. Chem. Eng. Data.* **2016**, 61, 1836-1849.
[70] Simmie, M, J.; Black, G.; Curran, J, H.; Hinde, P, J. Enthalpies of Formation and Bond Dissociation Energies of Lower Alkyl Hydroperoxides and Related Hydroperoxy and Alkoxy Radicals. *J. Phys. Chem. A.* **2008**, 5010-5016.
[71] Matthews, J.; Sinha, A.; Francisco, S, J.; Unimolecular dissociation and thermochemistry of CH_3OOH. *J. Chem. Phys*. **2005**, 122, 221101/1-221101/4.
[72] Li, Y.-M.; Sun, Q.; Li, H.-Y.; Ge, M.-F.; Wang, D.-X.; Characterization and Activity of CH_3OOH and CH_3CH_2OOH - Study on a Photoelectron Spectroscopy. *Chin. J. Chem*. **2015**, 23, 993-996.
[73] Faragó, E. P.; Szori, M.; Owen, M. C.; Fittschen, C.; Viskolcz, B.; Critical Evaluation of the Potential Energy Surface of the $CH_3 + HO_2$ Reaction System. *J. Chem. Phys*. **2015**, 054308/1-054308/11.
[74] Simmie, J. M.; Sheahan. J. N. Validation of a database of formation enthalpies and of mid-level model chemistries. *J. Phys. Chem. A.* **2016**, 120, 7370-7384.
[75] Blanksby, S. J.; Ramond, T. M.; Davico, G. E.; Nimlos, M. R.; Kato, S.; Bierbaum, V. M.; Lineberger, W. C.; Ellison, G. B.; Okamura, M. Negative-Ion Photoelectron Spectroscopy, Gas-Phase Acidity, and Thermochemistry of the Peroxyl Radicals CH_3OO and CH_3CH_2OO *J. Am. Chem. Soc.* **2001**, 123, 9585–9596.
[76] Agarwal, J.; Simmonett, C. A.; Schaefer, H. F. III.; Fundamental vibrational frequencies and spectroscopic constants for the methylperoxy radical, CH_3O_2, and related isotopologues $^{13}CH_3OO$, $CH_3{}^{18}O{}^{18}O$, and CD_3OO *Molecular Physics* **2012**, 110, 2419.
[77] Huang, D. R.; Chu, L. K.; Lee, Y. P. Infrared absorption of gaseous CH_3OO detected with a step-scan Fourier-transform spectrometer *J. Chem. Phys.* **2007**, 127, 234318.
[78] Niki, H.; Maker, P. D.; Savage, C. M.; Breitenbach, L. P. A Fourier transform infrared study of the kinetics and mechanism for the reaction hydroxyl + methyl hydroperoxide *J. Phys. Chem.* **1983**, 87, 2190-2193.
[79] Stathis, E.C.; Egerton; Note On Heats of Formation Of Peroxides. A. C. *Trans. Faraday. Soc.* **1940**, 36, 606-606.

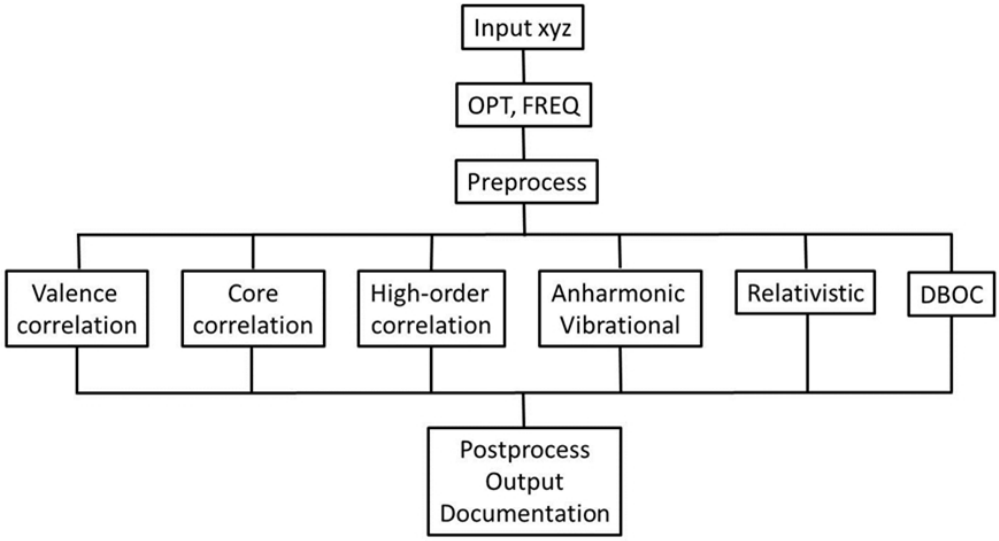

TOC

147x80mm (150 x 150 DPI)

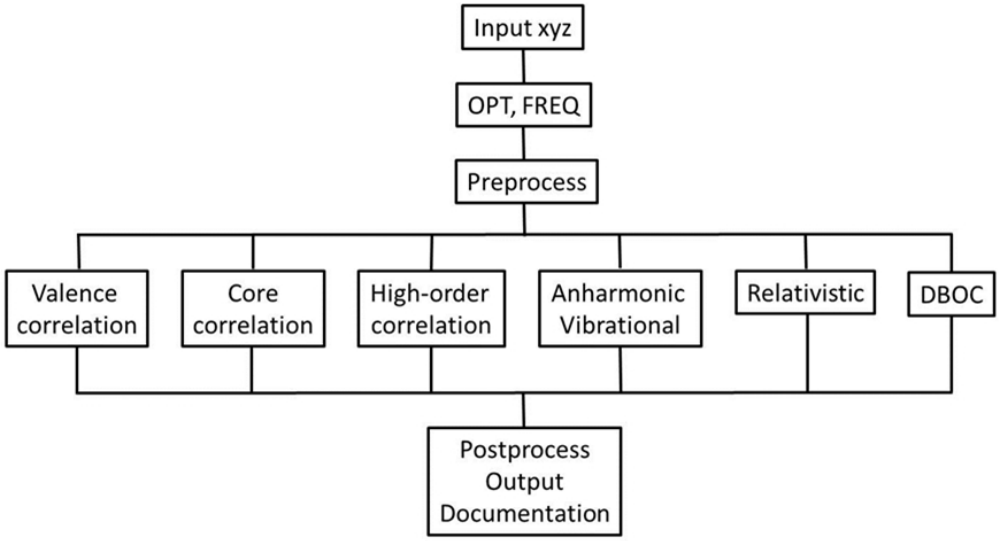

Figure 1: Flowchart of the automated thermochemical protocol. Details of each contribution to the composite energy and the pre- and post-processing procedures are given in the text.

147x80mm (150 x 150 DPI)

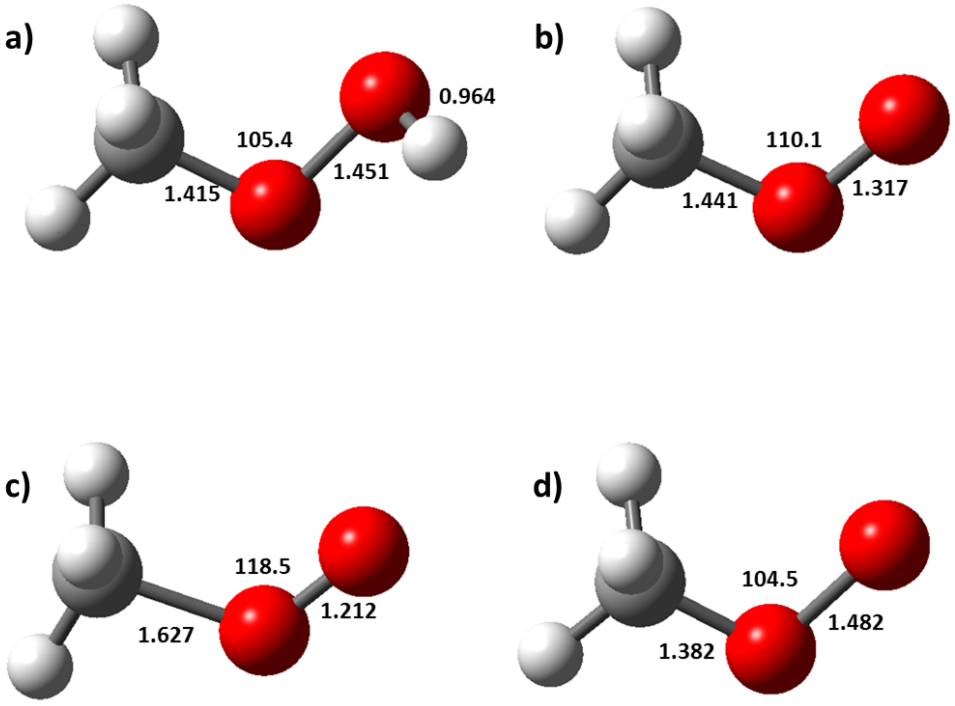

Figure 2: Some relevant structural parameters for members of the methylperoxy family (distances in Angstroms and angles in degrees). CH3O2 structures b), c) and d) are those of the neutral radical, cation, and anion systems, respectively.

175x132mm (150 x 150 DPI)

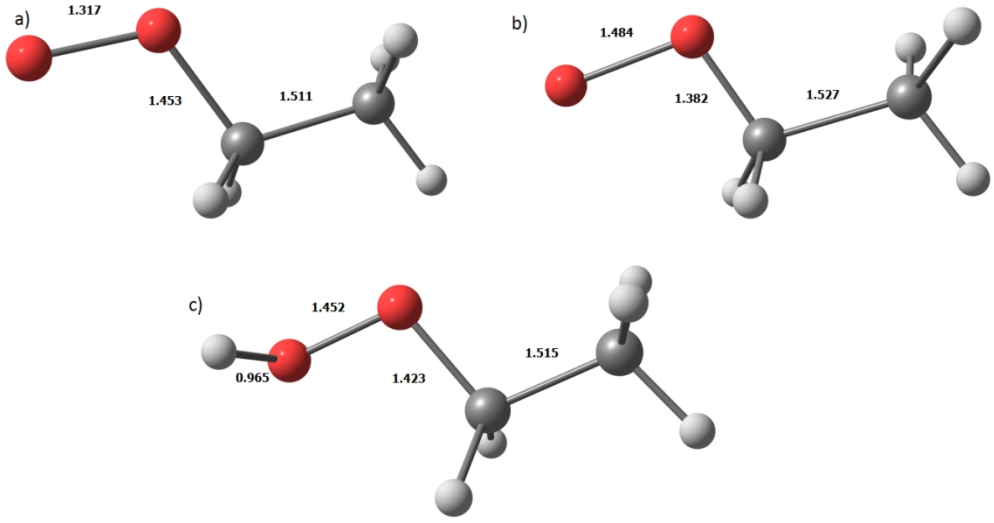

Figure 3: Some relevant structural parameters of the ethylperoxy and ethylhydroperoxide species; a) the radical, b) the anion, and c) the ethylhydroperoxide species.

354x186mm (96 x 96 DPI)